Available online at www.sciencedirect.com
ScienceDirect
Journal of the European Ceramic Society 29 (2009) 3371–3378
www.elsevier.com/locate/jeurceramsoc

Processing of ultrafine ZrO_2 toughened WC composites

Olivier Malek [a,b], Bert Lauwers [b], Yeczain Perez [c], Patrick De Baets [c], Jef Vleugels [a,*]

[a] K.U.Leuven, Department of Metallurgy and Materials Engineering, Kasteelpark Arenberg 44, B-3001 Leuven, Belgium
[b] K.U.Leuven, Department of Mechanical Engineering, Celestijnenlaan 300B, B-3001 Leuven, Belgium
[c] Universiteit Gent, Mechanical Construction and Production – Laboratory Soete, St.-Pietersnieuwstraat 41, B-9000 Gent, Belgium

Received 16 February 2009; received in revised form 15 June 2009; accepted 14 July 2009
Available online 8 August 2009

Abstract

The interrelationships between the dispersion of the secondary ZrO_2 phase and the material properties of WC-based composites with up to 10 vol% of ZrO_2 are investigated. The homogeneity of the ultrafine WC–nanometric ZrO_2 powder mixtures was optimized by means of multidirectional milling and bead milling. In an alternative route, zirconium butoxide was used as a ZrO_2 source. The composites were fully densified by means of pulsed electric current sintering (PECS), also known as spark plasma sintering, within a few minutes at 1700 °C allowing to maintain an ultrafine grained microstructure combining a hardness of 2600 kg/mm^2 with an indentation toughness of 6 MPa m$^{1/2}$. The ZrO_2 content and Y_2O_3 stabilization were found to strongly influence the mechanical properties and especially strength of the WC–ZrO_2 composites.

Keywords: PECS; Composites; Microstructure-final; Toughness and toughening; Carbides

1. Introduction

WC and WC-based cermets such as WC–Co are widely used in industry as cutting materials for steels due to their excellent wear performance. The addition of the Co metallic binder phase to the WC facilitates sintering and increases the mechanical properties of the composite considerably. In this research, the Co binder was replaced by 5 or 10 vol% ZrO_2. The utilization of ZrO_2 as a ceramic sinter additive instead of a metallic binder such as in WC–Co is particularly interesting because: (i) ZrO_2 is an electrical and thermal isolator, (ii) ZrO_2 does not soften at elevated temperatures, (iii) ZrO_2 is not susceptible to electrochemical corrosion and (iv) it is expected to increase the fracture toughness due to transformation toughening.[1] The envisaged application field for the developed WC–ZrO_2 composites are wear applications requiring a Vickers hardness well above 2000 kg/mm^2 in combination with a strength > 1000 MPa and acceptable toughness. More specifically, the application field of WC–Co materials in which the Co binder is a critical problem due to Co leaching in alkaline media or adhesion during metal extrusion or forming is addressed. The behaviour of ZrO_2 toughened Al_2O_3 has already been thoroughly investigated,[2,3] revealing that the addition of ZrO_2 particles enhances the fracture toughness and flexural strength considerably.

Earlier research was mainly focused on ZrO_2–WC composites with 40–60 vol% of zirconia revealing that composites prepared from nanometer-sized WC powders featured higher hardness, fracture toughness and strength than those prepared from micrometer-sized WC starting powders, when hot pressed at 1450 °C.[4] In addition, the optimal amount of Y_2O_3 stabilization for fracture toughness was found to be 2 mol%.[5] Full densification of WC–ZrO_2 composites with 15 vol% of 2 mol% Y_2O_3 stabilized ZrO_2 at 1300 °C using Spark Plasma Sintering (SPS) was reported[6] to result in a high hardness of 2450 kg/mm^2 and a fracture toughness of 5 MPa m$^{1/2}$. It is clear that the size and distribution of the ZrO_2 phase in the composite is of primary importance. In the present work, special attention was given to the influence of different milling and mixing methods and the effect they have on the composite mechanical properties. In order to obtain an even better dispersion of the ZrO_2 phase into the WC matrix, a metal alkoxide was used as a starting compound for ZrO_2.

2. Experimental procedure

For the primary bulk phase commercially available WC powder (grade CRC-015, Wolfram Bergbau und Hütten GmbH,

* Corresponding author at: Department MTM, Kasteelpark Arenberg 44 - bus 2450, 3001 Heverlee, Belgium. Tel.: +32 16 321244.
E-mail address: Jozef.Vleugels@mtm.kuleuven.be (J. Vleugels).

0955-2219/$ – see front matter © 2009 Elsevier Ltd. All rights reserved.
doi:10.1016/j.jeurceramsoc.2009.07.013

Austria) was used while the secondary ZrO_2 phase was composed of commercially available TZ-0 and TZ-3Y powders (Tosoh Corp., Japan). The required Y_2O_3-content was achieved by mixing Y_2O_3-free monoclinic powder (TZ-0) with co-precipitated 3Y-ZrO_2 powder (TZ-3Y). 5 and 10 vol% WC–ZrO_2 powders were wet mixed in ethanol in (a) a multidirectional Turbula mixer (TM, Type T2A, WAB, Basel, Switzerland) for 24 h at 70 RPM using 3 mm diameter WC–Co milling balls (Ceratizit grade MG15) or (b) a bead mill (BM, Dispermat SL, VMA Getzmann GmbH, Reichshof, Germany) using 1 mm diameter Y-TZP ZrO_2 milling beads (TZ-3Y, Tosoh Corp., Japan) at different rotation speeds (100, 1000 or 5000 RPM) for 30 min. The contamination from the WC–Co balls when using the Turbula was minimized due to the fact that mixing takes place in a low energy mode. The alkoxide route was explored as an alternative way to incorporate the ZrO_2 phase into the WC bulk using zirconium n-butoxide (80 wt.% $Zr[O(C_4H_9)]_4$ in n-butanol, ABCR GmbH & Co., Germany). The organic compound was treated under a protective nitrogen atmosphere and directly added to the bead milling ethanol based WC suspension together with a small amount of water to initiate hydrolysis. Y_2O_3 was provided in the form of yttrium nitrate, obtained by dissolving Y_2O_3 in HNO_3, which was added directly to the bead milling suspension. All samples feature 2 mol% Y_2O_3 stabilization unless stated otherwise. After Turbula mixing or bead milling, the suspension was dried in a rotating evaporator at 60 °C.

Pulsed electric current sintering (PECS) (Type HP D 25/1, FCT Systeme, Rauenstein, Germany) was performed in vacuum (4 Pa). A pulsed electric current with a pulse duration of 10 ms and pause time of 5 ms was applied throughout all sintering cycles. Pure WC or WC–ZrO_2 powder was poured into a cylindrical graphite die with an inner and outer diameter of 40 and 76 mm and sintered at 1550–1900 °C for 1.5–4 min. The heating rate was 300 °C/min from 450 to 1050 °C and subsequently 200 °C/min up to the sintering temperature. An initial cooling rate of 200 °C/min was obtained by switching off the power. The applied pressure was adjusted within 0.5 min from 16 to 30 MPa at 1050 °C and increased gradually from 30 to 60 MPa during the heating-up process from 1050 °C to the sintering temperatures. Graphite papers were used to separate the powder from the graphite die/punch set-up. To minimize the radiation heat loss from the graphite die wall, the die was surrounded with 10 mm thick porous carbon felt (Sigratherm Flexible carbon felt, SGL carbon group, Wiesbaden, Germany) insulation. A two-colour pyrometer (400–2300 °C, Impac, ChesterWeld, UK) was focused at the bottom of a central core hole in the upper punch, only 2 mm away from the top surface of the sample, to obtain a realistic sample temperature measurement. The actual set-up and temperature monitoring procedure is described in detail elsewhere.[7]

Density measurements were done in demineralised water. Phase identification was conducted by a θ–θ X-ray diffractometer (XRD, Seifert, Ahrensburg, Germany) using Cu Kα radiation (40 kV, 40 mA). Residual stresses are determined using X-ray diffraction on a Siemens D500 goniometer (Cu Kα source, 40 kV, 40 mA) applying the d-$\sin^2\psi$ method ((2 1 2) WC diffraction, $S_1 = -2.6667 \times 10^{-7}$ and $1/2S_2 = 1.56 \times 10^{-6}$). The microstructure of polished samples was investigated using Scanning Electron Microscopy (SEM, XL30-FEG, FEI, Eindhoven, The Netherlands). To assess the contamination level of the starting powders during bead milling, using Y-TZP ZrO_2 milling beads, Inductively Coupled Plasma-Optical Emission Spectrometry (ICP-AES, Liberty series II, Varian) was conducted according to the procedure described in literature.[8] The particle size distribution was measured by laser diffraction (Mastersizer Micro Plus, Malvern Instruments Ltd., UK) using the Mie Scattering method.

The Vickers hardness, HV_{10}, was measured on a hardness tester (Model FV-700, Future-Tech Corp., Tokyo, Japan) with an indentation load of 98.1 N for 15 s. The indentation fracture toughness, K_{IC}, was calculated from the length of the radial cracks according to the formula proposed by Anstis et al.[9] The reported hardness and fracture toughness are the mean and standard deviation of five indentations. The Young's modulus, E, of the pure WC and WC–ZrO_2 samples was measured on bars of 20 mm long using the resonance frequency, which was measured by the impulse excitation technique (Grindo-Sonic, J.W. Lemmens N.V., Leuven, Belgium). The flexural strength was measured on a 3-point bending test set-up (INSTRON 4467, Instron Corp., USA) with a span of 20 mm. A load cell of 5 kN and a loading rate of 0.1 mm/s were used. The bending bars were ground with a diamond grinding wheel (type D46SW-50-X2, Technodiamant, The Netherlands) on a Jung grinding machine (JF415DS, Jung, Germany). The reported strength data are the average and standard deviation of 7 bending bars. Sample cutting has been performed on a Wire-EDM machine, type Charmilles Robofil 240cc.

3. Results and discussion

3.1. Sintering temperature

The first step in this research was to determine the correct sintering temperature for WC–ZrO_2 composites using PECS (SPS). The goal was to reach a fully densified WC–ZrO_2 composite with optimal mechanical properties which can be used as a base material for further investigations. It is reported that binderless WC can be densified by PECS at 1900 °C.[10] However, the presence of ZrO_2 acts as a sintering additive, lowering the required temperature to achieve full densification considerably. Fig. 1 summarizes the density of the bead milled (BM, 100 RPM) 2 mol% yttria stabilized 5 and 10 vol% ZrO_2 grades PECS at 1550 (5 min), 1700 (4 min) and 1800 °C (2 min). The density of binderless WC PECS for 1.5 min at 1900 °C is given as a reference. The theoretical density was calculated by the rule of mixtures using a density of 15.26 g/cm^3 for WC and 6.05 g/cm^3 for ZrO_2. It is clear that full densification was achieved for 5 and 10 vol% ZrO_2 grades when PECS for 4 min at 1700 °C.

XRD patterns of the starting powder and the different PECS WC–10 vol% ZrO_2 grades are presented in Fig. 2. A survey of the ZrO_2 peaks indicates that the ZrO_2 phase in the starting powder was monoclinic whereas it was mainly tetragonal in all PECS

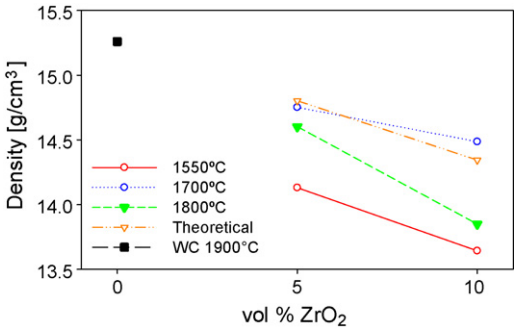

Fig. 1. Density of 100 RPM bead milled WC–ZrO_2 composites.

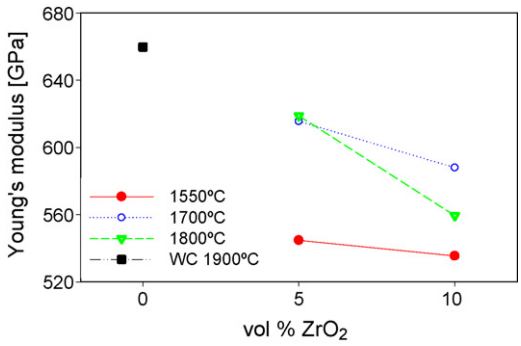

Fig. 3. Young's modulus of 100 RPM bead milled WC–ZrO_2 composites.

grades, independent of the PECS temperature. In addition, XRD also revealed the presence of ZrC and W_2C as reaction products in the PECS grades. Moskała and Pyda[11] already reported that when pressureless sintering for 1 h at ≥1750 °C, ZrC is formed from the reaction between WC and ZrO_2. This evolution is confirmed here. At 1550 °C, virtually no ZrC was present while there were clear peaks in the XRD measurements associated with ZrC at 1700 °C and 1800 °C. The formation of W_2C in the PECS WC grade indicates a substoichiometric carbon content in the WC powder. It is relatively hard to distinguish the W_2C and ZrC peaks due to overlap, but the strongest W_2C peak is located at 39.5° 2θ while the peak at 38.4° 2θ, which is associated with ZrC and weakly with W_2C, considerably increases with increasing PECS temperature. The peak at 39.5° 2θ remains relatively the same. This indicates that the amount of W_2C remained constant with increasing PECS temperature while the amount of ZrC increased. However, the difference between the 1700 °C and 1800 °C PECS grades with regard to ZrC content was relatively small. This can be explained by the fact that the formation of ZrC is not only temperature but also time dependent. To achieve full densification of the WC–ZrO_2 (90/10) grades, as measured by the dilatometer movement on the PECS equipment, 4 min was required at 1700 °C, whereas 2 min is sufficient at 1800 °C. The presence of ZrC and W_2C also implies the formation of CO_x during PECS. Due to the higher rate of densification at 1800 °C, it is expected that more CO_x remains trapped in the sample in the form of pores than at 1700 °C, explaining the slightly lower density (see Fig. 1). This also influences the mechanical properties, which are represented by the Young's modulus, hardness and fracture toughness (Fig. 3 and Table 1). The Young's modulus and hardness correlate with the density values, reported in Fig. 1. A high hardness up to 2400 kg/mm² and Young's modulus of 620 GPa accompany high density values for the 5 vol% ZrO_2 composite PECS at 1700 °C. A higher ZrO_2 content of 10 vol% leads to a higher fracture toughness up to 6 MPa $m^{1/2}$, compared to 4.9 MPa $m^{1/2}$ for pure WC. The ZrO_2 phase inhibits crack growth due to transformation toughening when transforming from the tetragonal to monoclinic phase in the stress field in front of the crack tip. This is shown in Fig. 4, comparing the XRD patterns of polished and fractured WC–ZrO_2 90/10 ceramics. The t-ZrO_2 peak clearly disappears in the fractured sample, indicating full transformation to m-ZrO_2. There is a small difference between the different sintering temperatures, mainly due to the fact that a residual porosity favourably influences the fracture toughness. Cracks can be stopped or hindered by the presence of pores explaining the slightly higher fracture toughness for

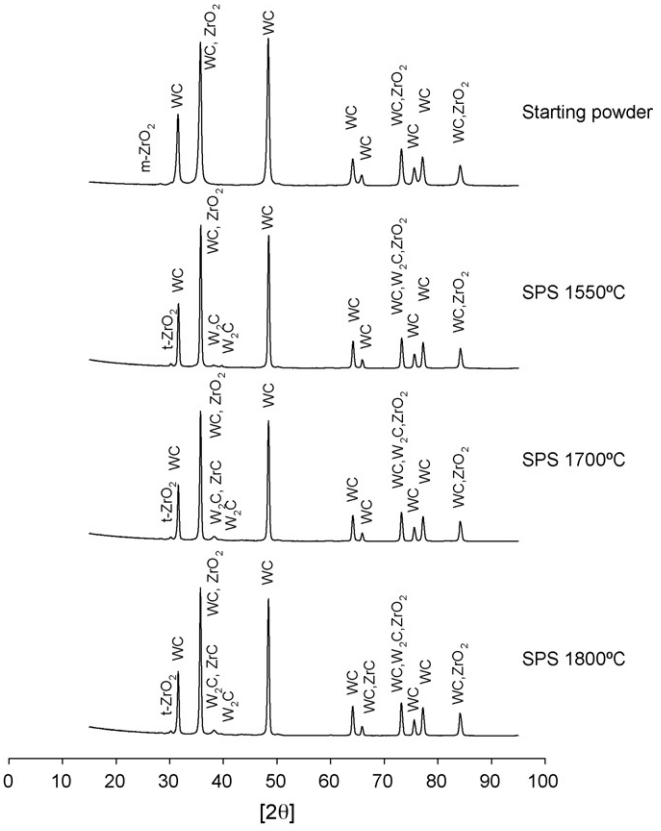

Fig. 2. XRD patterns of WC–ZrO_2 (90–10) composites.

Table 1
Vickers hardness and fracture toughness of 100 RPM bead milled WC–ZrO_2 composites.

ZrO_2 content [vol%]	PECS temperature [°C]	HV_{10} [kg/mm²]	K_{IC} [MPa $m^{1/2}$]
5	1550	1806 ± 14	6.0 ± 0.2
10	1550	1932 ± 73	6.0 ± 0.4
5	1700	2398 ± 19	5.4 ± 0.4
10	1700	2138 ± 40	5.8 ± 0.4
5	1800	2215 ± 58	5.7 ± 0.3
10	1800	1975 ± 25	6.2 ± 0.5
0	1900	2693 ± 41	4.9 ± 0.3

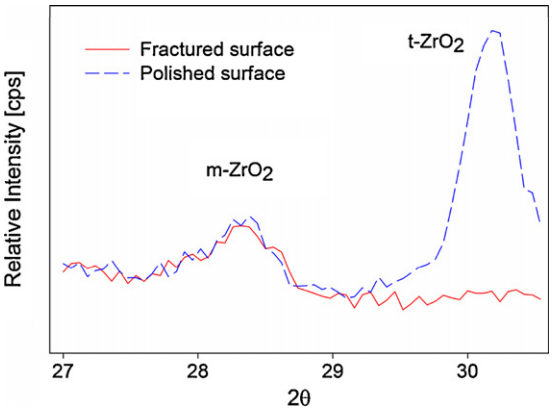

Fig. 4. XRD patterns of fractured and polished WC–ZrO_2 90/10 composites PECS at 1700 °C.

the 1550 °C and 1800 °C PECS grades. It can be concluded, based on the density and mechanical properties, that 1700 °C is the optimum PECS temperature for 2 mol% yttria stabilized WC–ZrO_2 composites with 5 or 10 vol% of ZrO_2, bead milled at 100 RPM.

3.2. ZrO_2 phase dispersion

SEM micrographs of polished Turbula mixed (TM) and bead milled (BM) powder based 10 vol% ZrO_2 composite grades PECS at 1700 °C are summarized in Fig. 5. Since bead milling at 100 RPM for 30 min resulted in residual ZrO_2 agglomerates with a size up to 20 μm in the densified composites, see Fig. 5a, the milling speed was increased to 1000 and 5000 RPM. Although the ZrO_2 agglomerate size can be reduced down to about 10 μm at 1000 RPM and 5 μm at 5000 RPM, agglomerates could not be completely avoided after 30 min of milling, as shown in Fig. 5c and d. Turbula mixing at 70 RPM for 24 h (Fig. 5b) resulted in a homogeneity that is comparable to that obtained after bead milling for 30 min at 1000 RPM. SEM analysis of the starting powders bead milled at 100 and 5000 RPM (see Fig. 5e and f) indicate that the average particle size did not alter, implying that the WC and ZrO_2 particle size of the starting powders was already too small to be further broken down using comminution by means of bead milling or Turbula mixing.

The density evolution of the bead milled composite grades PECS at 1700 °C is presented in Fig. 6. The density of the BM-

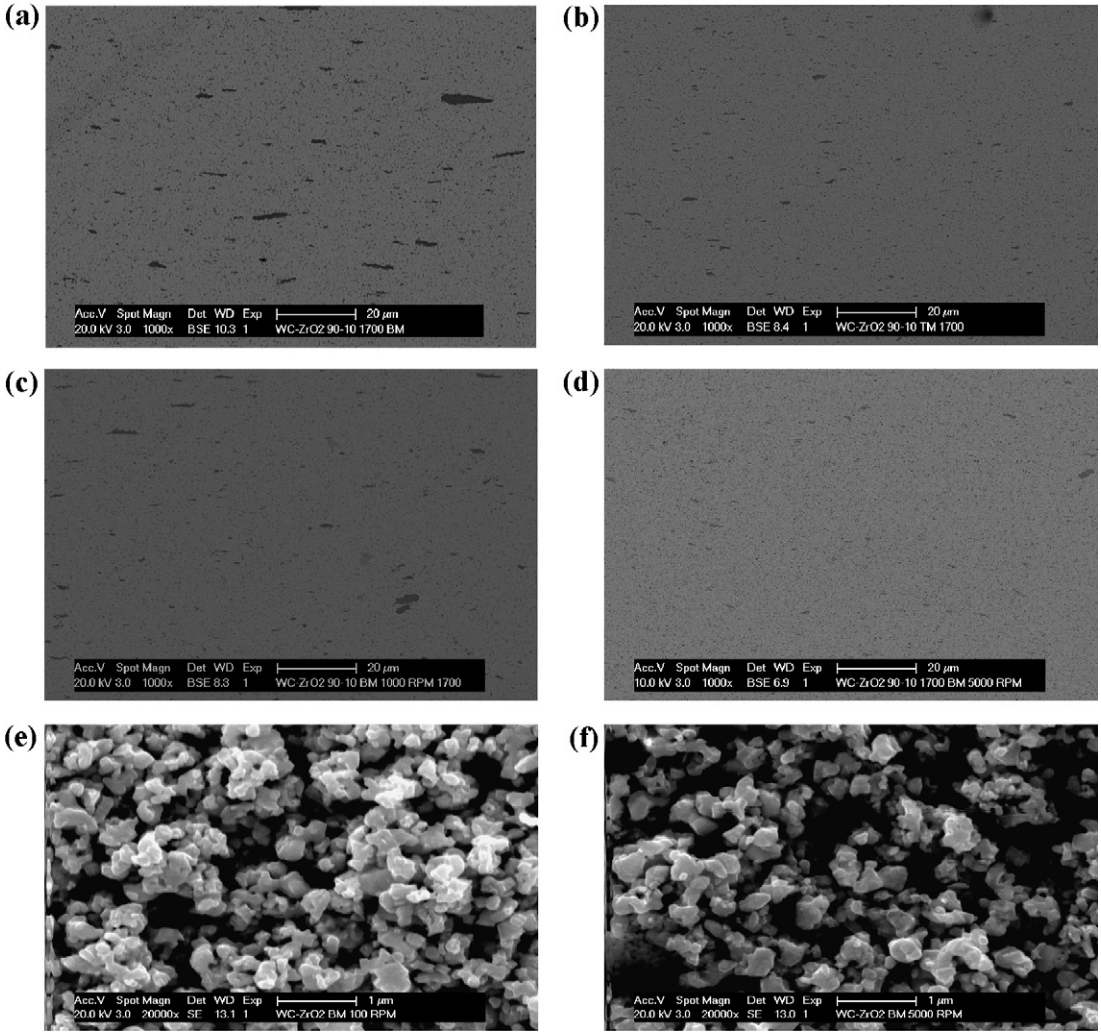

Fig. 5. Backscattered electron micrographs of WC–ZrO_2 (90/10) composites PECS at 1700 °C after Turbula mixing (b) or bead milling (a, c, and d for respectively 100, 1000 and 5000 RPM), and secondary electron micrographs of mixed starting powders bead milled at 100 RPM (e) or 5000 RPM (f).

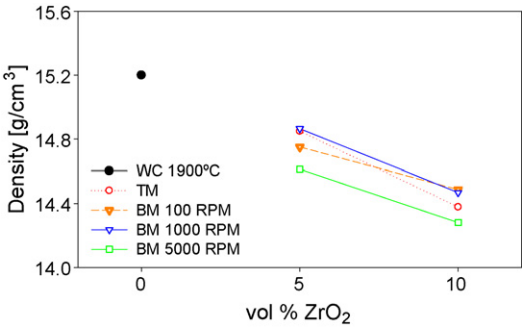

Fig. 6. Density of WC–ZrO_2 grades, PECS at 1700 °C.

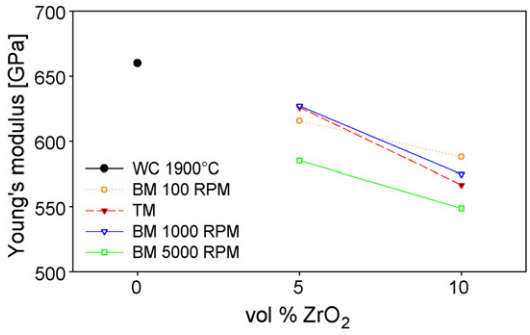

Fig. 7. Young's modulus of WC–ZrO_2 grades, PECS grades at 1700 °C.

5000 RPM grade is considerably lower than for BM-100 RPM, BM-1000 RPM and TM grades. A possible explanation could be a considerable amount of ZrO_2 contamination from the Y-TZP milling beads at the 5000 RPM high milling speeds. In order to assess this, ICP measurements were performed on the milled starting powders to determine the ZrO_2 content. The ICP measurements on the dissolved starting powder mixtures however showed no clear proof of any ZrO_2 contamination. ICP analysis revealed 9.5 and 9.8 vol% ZrO_2 for the TM and BM-5000 RPM WC–ZrO_2 (90/10) grades respectively, correlating very well with the targeted initial powder composition. ZrO_2 contamination can therefore be ruled out as a cause for the lower density of the BM-5000 RPM PECS grades.

Because the 2 mol% Y_2O_3 stabilization is achieved by mixing TZ-0 and TZ-3Y powders,[2,3] there is a possibility to overdisperse the m-ZrO_2 and 3Y-TZP powders inhibiting the Y_2O_3 stabilizer homogenisation during the fast thermal SPS cycle. The concomitant partial transformation and microcrack formation during cooling could then be a source of density loss. Therefore, WC–ZrO_2 (90/10) composites were prepared from 3 mol% Y_2O_3 stabilized co-precipitated ZrO_2 powder (Tosoh grade TZ-3Y) and bead milled at 1000 and 5000 RPM to assess the density evolution at higher RPM. However, a similar density drop was measured when increasing the bead milling speed from 1000 to 5000 using the 3 mol% Y_2O_3 co-precipitated ZrO_2 powder, eliminating the lack of local Y_2O_3 stabilization as a possible source for the reduced density.

A higher amount of ZrC and W_2C formed due to the increased ZrO_2/WC contact area at higher bead milling speed can be discarded because both W_2C and ZrC have a higher density than WC and ZrO_2 and their formation would not result in a lower overall density of the composite. In order to explain the reduced density of the SPS powders bead milled at 5000 RPM, the authors believe that the residual thermal tensile stresses in the ZrO_2 phase caused by the difference in thermal expansion between WC and t-ZrO_2 (5.20 and 10.9 μm/m °C respectively) are responsible for the spontaneous transformation of a fraction of highly dispersed ZrO_2 grains during cooling in the better dispersed materials obtained at higher bead milling speed.

The dwell time at the sintering temperature to obtain full density, as measured by the movement of the upper punch during PECS, changed considerably under the influence of the higher homogeneity of the starting powders. For a BM-100 RPM WC–ZrO_2 (90/10) composite, full density was obtained after 4 min of PECS at 1700 °C, whereas only 2.5 min was needed for the BM-5000 RPM grades and 3 min for the BM-1000 RPM and TM grades. The reason for this is that ZrO_2 is a more effective sintering aid when the agglomerates are removed. The observation that the ZrC content in the PECS grades is both temperature and time dependent is confirmed here. Due to the considerably lower dwell times in the TM, BM-1000 RPM and BM-5000 RPM 1700 °C PECS grades, almost no ZrC could be found by means of XRD measurements. The amount of W_2C was constant.

The mechanical properties of the composites PECS at 1700 °C are summarized in Fig. 7 and Table 2. The lower density of the BM-5000 RPM grades influences the Young's modulus and hardness negatively, as expected. The BM-1000 RPM grades provide the best combination of density, hardness and toughness, but are only marginally better than the TM grades. From Fig. 4 it is clear that the amount and size of ZrO_2 agglomerates has been reduced significantly by increasing the bead milling (30 min) rotation speed to 1000 RPM or switching to Turbula mixing for 24 h. A more homogenous dispersion of ZrO_2 in the bulk led to a higher hardness (2580 ± 59 kg/mm^2) as well as fracture toughness (6.2 ± 0.3 MPa m$^{1/2}$) for BM-1000 RPM PECS at 1700 °C. However, bead milling at very high milling speeds of 5000 RPM appeared not to be suitable for PECS using 3 mol% Y_2O_3 sta-

Table 2
Vickers hardness and fracture toughness of WC–ZrO_2 composites PECS at 1700 °C.

ZrO_2 content [vol%]	Milling method	HV_{10} [kg/mm^2]	K_{IC} [MPa m$^{1/2}$]
5	BM-100 RPM	2398 ± 19	5.4 ± 0.4
10	BM-100 RPM	2138 ± 40	5.8 ± 0.4
5	TM	2514 ± 48	5.1 ± 0.1
10	TM	2218 ± 31	5.9 ± 0.3
5	BM-1000 RPM	2581 ± 60	6.1 ± 0.3
10	BM-1000 RPM	2312 ± 34	6.2 ± 0.3
5	BM-5000 RPM	2330 ± 18	5.2 ± 0.3
10	BM-5000 RPM	2299 ± 44	5.5 ± 0.2
5 butoxide	BM-5000 RPM	2539 ± 28	5.6 ± 0.3
10 butoxide	BM-5000 RPM	2243 ± 27	5.8 ± 0.4
5 butoxide 2Y	BM-5000 RPM	2602 ± 60	5.5 ± 0.5
10 butoxide 2Y	BM-5000 RPM	2475 ± 14	6.1 ± 0.2
WC	–	2693 ± 41	4.9 ± 0.3

bilized co-precipitated ZrO_2 (TZ-3Y) as well as mixtures of Y_2O_3-free monoclinic (TZ-0) and TZ-3Y powder.

3.3. Zirconium alkoxide as ZrO_2 precursor

It can be concluded from the previous section that a higher homogeneity of the composite increases the mechanical properties considerably. For this reason it is interesting to investigate the possibility to introduce the ZrO_2 at a molecular level into the WC starting powder. This can be achieved by adding zirconium butoxide (BUT) to a WC suspension. The butoxide will be homogenously dispersed in the WC suspension and hydrolyse in the presence of added water (reaction (1)). The zirconium hydroxides will graft to the WC particle surface and will be in situ converted to ZrO_2 during the thermal PECS cycle, as represented in reaction (2). The alkoxide can also be directly converted into a pure oxide powder during thermal degradation according to reaction (3):

$$Zr[OC_4H_9]_4 + 4H_2O \rightarrow Zr(OH)_4 + 4C_4H_9OH \quad (\text{at RT}) \quad (1)$$

$$Zr(OH)_4 \rightarrow ZrO_2 + 2H_2O \quad (2)$$

$$Zr[OC_4H_9]_4 \rightarrow ZrO_2 + 2C_4H_9OH + 2C_4H_8 \quad (\text{at } 325\text{–}500\,^{\circ}\text{C}) \quad (3)$$

A clear drop in the vacuum level during PECS was observed at 600 °C, indicating the removal of gas from the powder, as illustrated in Fig. 8. TGA measurements of alkoxide precursor based WC–ZrO_2 80/20 starting powder revealed that the powder is losing up to 25% of weight when heating to 500 °C, the temperature at which oxidation occurs in air. The removal of

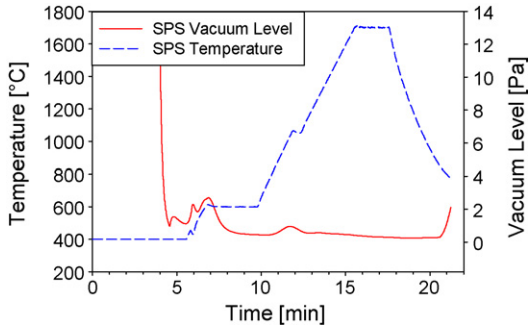

Fig. 8. Pressure and temperature curves during PECS of Zr-butoxide based WC–ZrO_2 90/10 powder mixtures.

remaining organic compounds and moisture are the cause for the decreased vacuum during PECS.

It is anticipated that when the ZrO_2 phase can be homogenously dispersed in the WC matrix and the grain size after PECS is below the critical size for maintaining nanometric t-ZrO_2, the presence of Y_2O_3 as ZrO_2 phase stabilizer might no longer be required. For this reason the samples were also produced without Y_2O_3 stabilizer. Composite grades were bead milled at 5000 RPM and PECS at 1700 °C. SEM micrographs, shown in Fig. 9, indicate the creation of a nearly perfect homogenous composite without ZrO_2 agglomerates. In addition, the majority of ZrO_2 grains are located at the triple points in the WC matrix. The ZrO_2 grains created by the alkoxide precursor range from 20 to 200 nm with an average of 75 nm, as measured by FEG-SEM analysis (see Fig. 9b). The ZrO_2 grains are significantly smaller than the 0.5 μm sized WC grains (Fig. 9c). The measured average WC particle size in the densified composites corresponds with the starting powder particle size distribution (0.51 μm), indicating that no WC grain growth occurred during PECS.

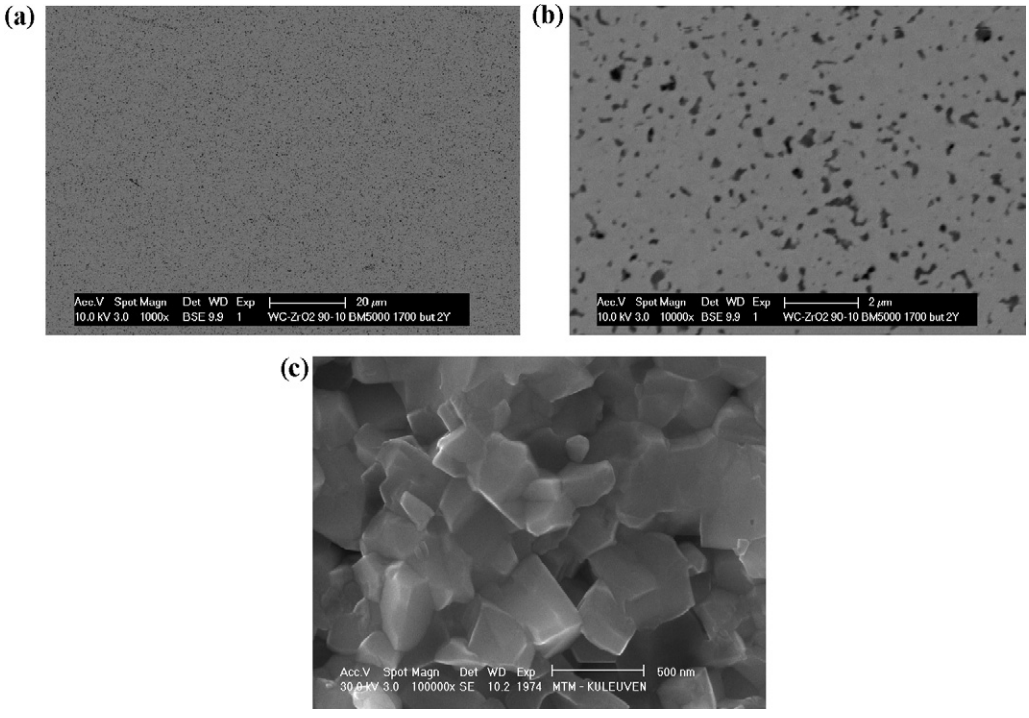

Fig. 9. Scanning Electron Micrographs of polished (a, b) and fractured (c) WC–ZrO_2 90/10 butoxide grades, PECS at 1700 °C.

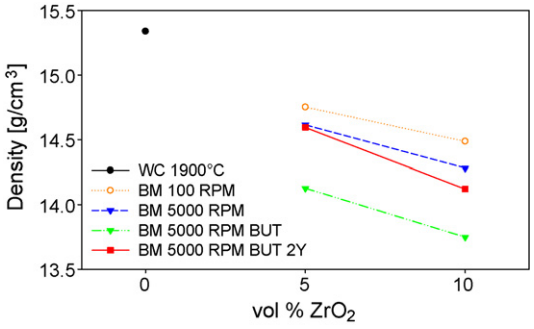

Fig. 10. Density of WC–ZrO_2 grades PECS at 1700 °C.

The influence of the use of the alkoxide precursor on the density is shown in Fig. 10. The density of the 2 mol% Y_2O_3 doped grade BM-5000 RPM BUT 2Y was similar as for the 5000 RPM bead milled ZrO_2 powder based composites. Without Y_2O_3 stabilization however, the density dropped to about 95% of the theoretical value. The reason for this has to be found in the transformation from tetragonal to monoclinic phase of the ZrO_2 during cooling. The XRD patterns of polished Y_2O_3 free and doped butoxide based composites are compared in Fig. 11, revealing that Y_2O_3 was required to maintain a tetragonal ZrO_2 phase after cooling. The volumetric expansion of the ZrO_2 during transformation, accompanied by microcrack formation, lowered the density. In addition, a drop of the required dwell time to reach full densification during PECS to 2 min was observed, confirming the earlier suggestion that a finer ZrO_2 particle size increases densification. The 2 mol% Y_2O_3 stabilized composite showed a superior hardness of 2475 ± 16 kg/mm^2 and *E*-modulus of 583 GPa, with an acceptable fracture toughness of 6.1 ± 0.2 MPa m$^{1/2}$ for 10 vol% ZrO_2 composite, as shown in Fig. 12 and Table 2. The spontaneous transformation from t- to m-ZrO_2 in the samples without Y_2O_3 stabilization resulted not only in a lower stiffness, hardness and density but also a reduced flexural strength. A considerably higher flexural strength of 1536 ± 131 MPa was measured for the 2 mol% yttria stabilized WC–ZrO_2 (90/10) grade compared to 1210 ± 100 MPa for the non-stabilized grade, as shown in Fig. 13. X-ray diffraction measurements of ground bending bar surfaces revealed high residual compressive stresses of 1.78 ± 0.08 and 1.87 ± 0.08 GPa in the

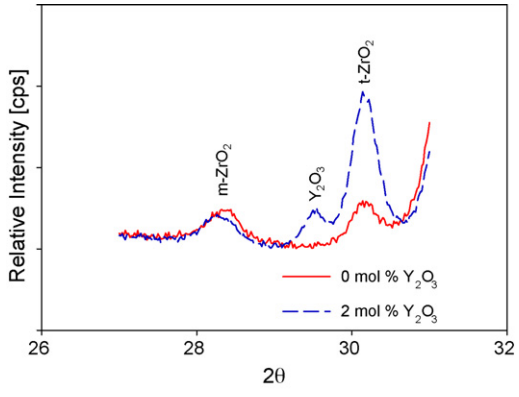

Fig. 11. XRD patterns of polished WC–ZrO_2 90/10 butoxide grades with and without Y_2O_3 addition, PECS at 1700 °C.

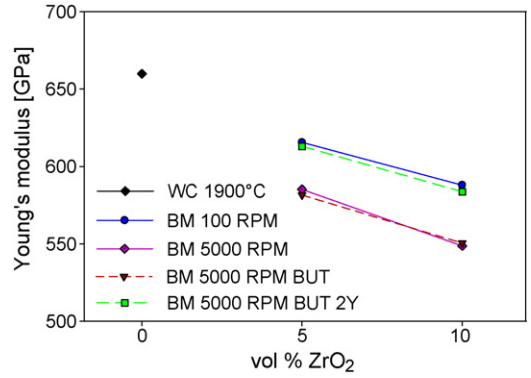

Fig. 12. *E*-modulus of WC–ZrO_2 composites PECS at 1700 °C.

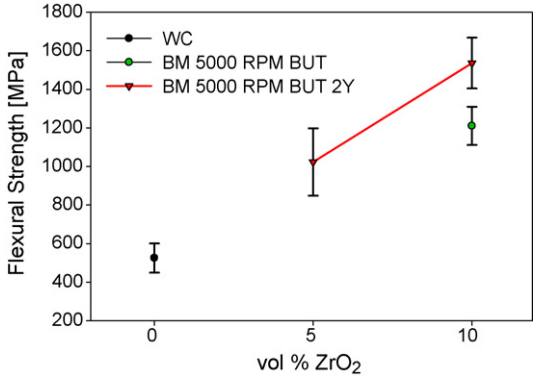

Fig. 13. Flexural strength of WC–ZrO_2 composites PECS at 1700 °C.

WC phase for the non-stabilized and 2 mol% yttria stabilized alkoxide based WC–ZrO_2 (90/10) grades PECS at 1700 °C. These high compressive stresses are beneficial for the flexural strength and effectively aid in preventing crack formation at the surface. The absence of agglomerates and the extremely small grain size of the ZrO_2 particles in the butoxide grades enhanced their hardness and Young's modulus considerably compared to the BM-5000 RPM ZrO_2 powder based grades with comparable ZrO_2 content (see Fig. 12 and Table 2). It can be concluded that increasing the homogeneity by means of zirconium-butoxide precursor provides superior mechanical properties compared to composites based on classical powder mixing.

4. Conclusions

WC–ZrO_2 powder mixtures with 5 or 10 vol% of 2 mol% Y_2O_3 stabilized ZrO_2, bead milled for 30 min at 100 RPM, can be fully densified using Pulsed Electric Current Sintering at 1700 °C with a dwell time of 4 min. XRD measurements indicate the formation of ZrC and W_2C as side products. Bead milling at low rotation speeds results in residual ZrO_2 agglomerates of up to 20 μm which can be decreased in size by increasing the bead milling speed up to 1000 or 5000 RPM during 30 min or multidirectional mixing for 24 h. The higher starting powder homogeneity improves the densification during PECS and allows to completely eliminate the formation of ZrC by a reduced dwell time at the sintering temperatures. The optimal

bead milling speed for PECS at 1700 °C using ZrO_2 powder mixtures is found to be 1000 RPM.

A homogenous ZrO_2 distribution can be realised using a liquid zirconium-butoxide precursor. The grain size after densification however is not small enough to avoid spontaneous transformation after sintering and 2 mol% Y_2O_3 stabilizer is essential to stabilize the t-ZrO_2 phase. The zirconium-butoxide precursor method with the addition of Y_2O_3 in the form of yttrium nitrate creates a homogenous 2 mol% Y_2O_3 stabilized composite which avoids spontaneous transformation associated with a too high dispersion of the ZrO_2 phase when using ZrO_2 powder mixtures.

The addition of ZrO_2 in the form of a zirconium-butoxide precursor to the WC matrix increases the fracture toughness from $4.9 \pm 0.3\,\text{MPa}\,\text{m}^{1/2}$ for pure WC to 5.5 ± 0.8 and $6.1 \pm 0.2\,\text{MPa}\,\text{m}^{1/2}$ for respectively 5 and 10 vol% of 2 mol% Y_2O_3 stabilized ZrO_2. This has been accomplished without decreasing the hardness significantly. The reason for this is the homogenous distribution of the ZrO_2 phase in the WC matrix. A high hardness of 2602 ± 61 and $2474 \pm 16\,\text{kg/mm}^2$ has been measured for respectively 5 or 10 vol% of 2 mol% Y_2O_3 stabilized ZrO_2. The toughening effect of the ZrO_2 is accompanied with a large increase in flexural strength from 570 ± 16 MPa for pure WC up to 1536 ± 131 MPa for WC–ZrO_2 (90/10) composites PECS at 1700 °C. It can be concluded that the addition of small amounts of ZrO_2 leads to an acceptable fracture toughness and significantly higher flexural strength without sacrificing hardness.

Acknowledgements

This work was financially supported by Project No. G.0539.08 of the Fund for Scientific Research Flanders (FWO). The authors wish to thank Bram Neirinck for the helpful suggestions to dissolve the composite powders for ICP measurements.

References

1. Basu, B., Ventkateswaran, T. and Sarkar, D., Pressureless sintering and tribological properties of WC–ZrO_2 composites. *J. Eur. Ceram. Soc.*, 2005, **25**, 1603–1610.
2. Tuan, W. H., Chen, R. Z., Wang, T. C., Cheng, C. H. and Kuo, P. S., Mechanical properties of Al_2O_3/ZrO_2 composites. *J. Eur. Ceram. Soc.*, 2002, **22**, 2827–2833.
3. Basu, B., Vleugels, J. and Van der Biest, O., ZrO_2–Al_2O_3 composites with tailored toughness. *J. Alloys Compd.*, 2004, **372**, 278–284.
4. Huang, S. G., Vanmeensel, K., Van der Biest, O. and Vleugels, J., Development of ZrO_2–WC composites by pulsed electric current sintering. *J. Eur. Ceram. Soc.*, 2007, **27**, 3269–3275.
5. Jiang, D., Vleugels, J. and Van der Biest, O., ZrO_2–WC nanocomposites with superior properties. *J. Eur. Ceram. Soc.*, 2007, **27**, 1247–1251.
6. Basu, B., Lee, J. and Kim, D., Development of WC–ZrO_2 nanocomposites by spark plasma sintering. *J. Am. Ceram. Soc.*, 2004, **87**, 317–319.
7. Vanmeensel, K., Laptev, A., Hennicke, J., Vleugels, J. and Van der Biest, O., Modelling of the temperature distribution during field assisted sintering. *Acta Mater.*, 2005, **53**, 4379–4388.
8. Archer, M., McCrindle, R. I. and Rohwer, E. R., Analysis of cobalt, tantalum, titanium, vanadium and chromium in tungsten carbide by inductively coupled plasma-optical emission spectrometry. *JAAS Tech. Note*, 2003, **8**, 1493–1496.
9. Anstis, G. R., Chantikul, P., Lawn, B. R. and Marshall, D. B., A critical evaluation of indentation techniques for measuring fracture toughness. I. Direct crack measurements. *J. Am. Ceram. Soc.*, 1981, **64**, 533–538.
10. Huang, S. G., Vanmeensel, K., Van der Biest, O. and Vleugels, J., Binderless WC and WC–VC materials obtained by pulsed electric current sintering. *Int. J. Refract. Met. Hard Mater.*, 2008, **26**, 41–47.
11. Moskała, N. and Pyda, W., Thermal stability of tungsten carbide in 7 mol.% calcia–zirconia solid solution matrix heat treated in argon. *J. Eur. Ceram. Soc.*, 2006, **26**, 3845–3851.